Separation Science and Technology
Publication details, including instructions for authors and subscription information:
http://www.informaworld.com/smpp/title~content=t713708471

Separation of Isomeric Xylenes: Experimental and Modeling

Toraj Mohammadi[a]; Mehrnaz Peivasti Rezaeian[a]
[a] Research Lab for Separation Processes, Department of Chemical Engineering, Iran University of Science and Technology, Narmak, Tehran, Iran

To cite this Article Mohammadi, Toraj and Rezaeian, Mehrnaz Peivasti(2009) 'Separation of Isomeric Xylenes: Experimental and Modeling', Separation Science and Technology, 44: 4, 817 — 840
To link to this Article: DOI: 10.1080/01496390802697072
URL: http://dx.doi.org/10.1080/01496390802697072

Separation Science and Technology, 44: 817–840, 2009

ISSN: 0149-6395 print/1520-5754 online
DOI: 10.1080/01496390802697072

Taylor & Francis
Taylor & Francis Group

Separation of Isomeric Xylenes: Experimental and Modeling

Toraj Mohammadi and Mehrnaz Peivasti Rezaeian
Research Lab for Separation Processes, Department of Chemical Engineering, Iran University of Science and Technology, Narmak, Tehran, Iran

Abstract: In this research, mass transport in pervaporation (PV) process of isomeric xylenes (para_xylene and ortho_xylene) was investigated by means of the resistances-in-series model. In order to obtain necessary data for the analysis, some experimental studies on separation of the xylene mixtures using a poly (vinyl alcohol) (PVA) membrane were performed. Influence of operating conditions such as para_xylene concentration in the feed and permeate pressure on the membrane performance and also the transport resistances in different layers of membrane was examined. Finally, the impact of CBr_4 (Carbon tetrabromide) on the membrane performance was evaluated. The results implied that by adding CBr_4 to the feed, more ortho_xylene in the permeate can be collected, because CBr_4 combines with para_xylene molecules, thus ortho_xylene molecules preferably pass through the membrane rather than para-xylene molecules. The mathematical model was found to be very accurate and could be employed for prediction of PV of isomeric xylenes.

Keywords: CBr_4, isomeric xylenes, pervaporation, resistances-in-series model

INTRODUCTION

Xylenes are one of the most important chemicals, which are mainly used for the production of motor fuels and many other chemicals such as

Received 26 April 2008; accepted 13 November 2008.
Address correspondence to Toraj Mohammadi, Research Lab for Separation Processes, Department of Chemical Engineering, Iran University of Science and Technology, Narmak, Tehran, Iran. Fax: 0098 21 77240495. E-mail: torajmohammadi@iust.ac.ir

terephthalic acid, phthalic anhydride, isophthalic acid, etc. Since xylenes are always produced as a mixture of isomers, the separation of xylene isomers is an important process in the production of pure xylenes. Partial vaporization of a liquid through a dense polymeric membrane is called pervaporation. Compared with distillation, pervaporation can be considered a better candidate for separation of close boiling, azeotropic or isomeric mixtures. For removal of volatile organic compounds, other separation technologies such as distillation, liquid-liquid extraction, carbon/zeolite adsorption and air stripping are not applicable due to limitations of feed conditions, large volume of byproducts, and/or high cost of required post-treatments. However, pervaporation can be applied without these limitations (1). Currently, most commercial pervaporation processes involve dehydration of alcohols and other organic solvents, or recovery of organic solvents from dilute aqueous systems. Pervaporation is today considered as a basic unit operation for separation of organic–organic liquid mixtures because of its efficiency in separating azeotropic and close-boiling mixtures, isomers, and heat-sensitive compounds (2). Many researchers have worked on separation of isomers such as J. Sikonia et al., who performed amodification of poly (vinylidene fluoride) membranes by inccorporating Werner complexes in them for separation of the xylene isomers (3). Also, the paper by Wegner et al. reports experimental results on pervaporation of pure xylene isomers and their binary mixtures through alumina-supported zeolite MFI membranes (4). Takaba et al. have researched on separation of isomeric xylenes using cyclodextrin-modified ceramic membranes (5). Another research has been done on separation of isomeric xylenes through PVA membrane filled β-cyclodextrin by which our results were compared and analyzed (6).

It has to be mentioned that in the present work the xylene mixture purchased from Isfahan Petrochemical Co. contains only ortho/para_xylene, which is separated by a conventional method using zeolites (Parex^{TM} process, UOP Company, USA). Thus, it was decided just to separate the ortho/para mixture in this study. Also, since para_xylene is currently in greatest demand in petrochemical industries, the recovery of para_xylene is preferable rather than ortho_xylene.

The performance of PV is usually assessed using permeation flux and separation factor which are affected by the transport mechanisms and by the operating conditions (7). Much attention has been paid to modeling of PV membranes and, with increasing industrial applications, to modeling of PV systems. Modeling of mass transport in PV systems can be simply studied by applying the resistance-in-series model which allows the calculation of mass transport resistances in the liquid feed boundary layer and in the composite membrane (8). Apart from its simplicity, the

model allows for the contribution of the boundary layer and the membrane resistances to be separated and analyzed (7).

For modeling of PV, permeation flux and separation factor affected by solubility and diffusivity of constituents in the membrane have to be obtained. Traditionally, the solubility was calculated according to the Flory-Huggins theory. However, the interaction parameter χ which depends on temperature and concentration strongly has to be determined experimentally. This can limit its predictive capacity. Recently, group contribution methods have been successfully applied to predict activity coefficients in polymer solutions (9). However, in this case, the separation of isomers, UNIFAC model can not be employed lonely for estimating of activities, because this model does not distinguish between the groups of isomers and both isomers sound the same according to this model. Thus a new method, on the basis of both the Flory-Huggins theory and UNIFAC model, was applied for modeling of the solubility in the PVA composite membrane.

Moreover, an approach based on the idea to make a complex with one of the isomers to render it less permeable through the membrane was investigated (10). Thus, the separation of ortho_xylene and para_xylene isomers in the presence of CBr_4, which selectively forms a complex with para_xylene at certain concentrations and temperatures, was considered here.

The work described in this article is based on the earlier researches of Jiraratananon and Huang (2001) (7), who studied the transport through a dense membrane, and the solution-diffusion model to account for describing fluxes of components. The objectives of this work are to analyze the transport resistances and to estimate the fluxes of constituents in the composite membrane.

THEORY

Modeling of Mass Transport Through the Membrane

In general, membrane separation processes are effective, if they have relatively high separation factors and permeation fluxes which both depend on mass transport mechanism and operating conditions. Regarding mass transport mechanism; it has to be noted that it is important how permeants diffuse through the feed bulk and the membrane, and regarding the operating conditions; hydrodynamic conditions and system geometries have the most importance. Based on the resistance-in-series model, transport resistances against a constituent passing through the membrane are considered by the following steps (it has to be noted that the mass

transfer resistance on the vapor side is usually considered to be negligible). The concentration profile of the components for a binary system is depicted in Fig. 1 (7).

Transport Through the Liquid Boundary Layer

The diffusive flux of i through a liquid boundary layer can be expressed by the following equation:

$$J_i = k_{bl}\rho_L(x_{i,L} - x_{i,LM}) \tag{1}$$

In the boundary layer, the sum of convective transport ($V_P\, x_{i,L}$) and diffusive transport $\left(-D_{i,L}\frac{dx_{i,L}}{dz}\right)$ equals the amount of permeation through the membrane, i.e.:

$$V_p x_{i,L} - D_{i,L}\frac{dx_{i,L}}{dz} = V_p x_{i,p} \tag{2}$$

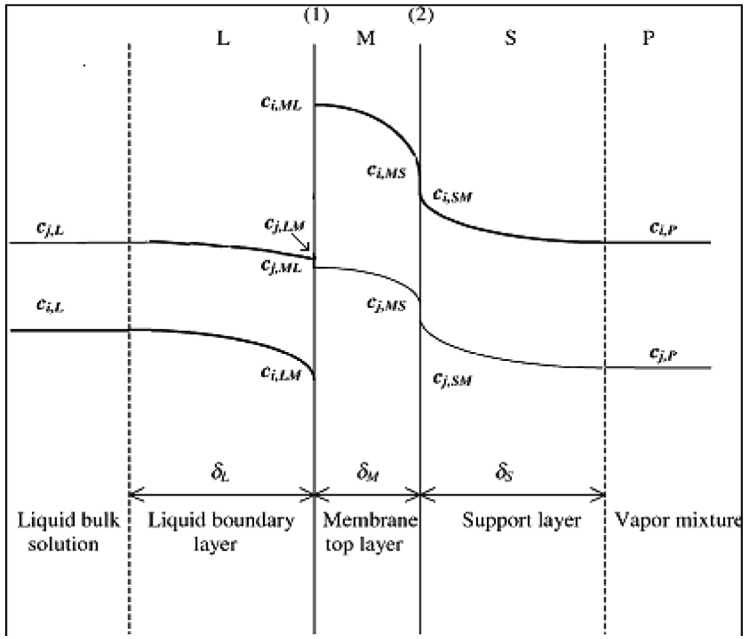

Figure 1. Concentration profile across the membrane for a binary system.

This equation can be integrated over the thickness of the boundary layer to give the well-known concentration polarization equation:

$$\frac{x_{i,m} - x_{i,P}}{x_{i,b} - x_{i,P}} = \exp\left(\frac{V_P}{k_{bl}}\right) \tag{3}$$

Where k_{bl} equals to $D_{i,L}/\delta$ in which δ is the thickness of boundary layer.

$$\frac{1/\beta_\circ - 1}{1/\beta - 1} = \exp\left(\frac{V_P}{k_{bl}}\right) \tag{4}$$

Where, β and $\beta_\circ$ are defined as $\frac{x_{i,P}}{x_{i,b}}$ and $\frac{x_{i,P}}{x_{i,m}}$, respectively.

To incorporate the contribution of convective transport, one can replace Eq. (1) by the concentration polarization Eq. (3), which can be rearranged to give:

$$J_i = \frac{\rho_L V_p}{(1 - (1/\beta_i))\left[\exp(V_\mathrm{p}/k_{bl}) - 1\right]}(x_{i,L} - x_{i,LM}) \tag{5}$$

Thus, with regards to, $x_i = \frac{a_i}{\gamma_i}$ the mass transport resistance in the liquid boundary layer equals to:

$$R_{i,L} = \frac{(1 - (1/\beta_i))[\exp((V_P/k_{bl}) - 1)] \cdot \gamma_{i,L}}{V_P \rho_L} \tag{6}$$

Diffusion into the Membrane Top Layer

Fick's first law of diffusion is applied to describe the diffusion of a component in the membrane top layer:

$$J_i = D_{iM} \cdot \frac{dc_{i,M}}{dz} \tag{7}$$

Depending on how the diffusion coefficient is expressed, this equation is changed.

Burn et al. proposed the exponential diffusion equations which include effects of plasticizing and coupling on the diffusivities (11):

$$D_{i,M} = D^0_{i,M} \exp(k_{ii} \cdot c_i + k_{ij} \cdot c_j) \tag{8}$$

If Eq. (8) is incorporated into the Eq. (7), we can write:

$$J_i = D^0_{i,M} \exp(k_{ii} c_i + k_{ij} c_j) \frac{dc_{i,M}}{dz} \tag{9}$$

After integration, we have:

$$J_i = \frac{D^0_{i,M}}{\delta_M} \int \left(\exp(k_{ii}c_i + k_{ij}c_j)\right) dc_{i,M} \tag{10}$$

The right hand side of the above equation is manipulated and divided by $(c_{i,ML} - c_{i,MS})$:

$$J_i = \frac{D^0_{i,M}}{\delta_M} \times \left(\frac{1}{c_{i,ML} - c_{i,MS}}\right) \times (c_{i,ML} - c_{i,MS}) \int (\exp(k_{ii}c_i + k_{ij}c_j)) dc_{i,M} \tag{11}$$

We set

$$A = \frac{D^0_{i,M}}{\delta_M} \times \left(\frac{1}{c_{i,ML} - c_{i,MS}}\right) \times \int \left(\exp(k_{ii}c_i + k_{ij}c_j)\right) dc_{i,M}$$

And we have $c_{i,MS} = K_{si} \cdot a_{i,SM}$ and $c_{i,ML} = K_{si} \cdot a_{i,LM} \rightarrow J_i$

$$= AK_{si}(a_{i,LM} - a_{i,SM}) \tag{12}$$

Thus, the membrane top layer resistance equals to:

$$R_{i,M} = \frac{1}{AK_{si}} \tag{13}$$

Transport of Vapor Molecules Through the Porous Support of PVA Membrane

The PVA membrane used here is consisted of a support layer which has two separated layers (Non-woven fabric layer which is made of compacted fibers with an equivalent pore size of 20 micro meters and PAN layer with an equivalent pore size of 20 nano meters). If the amount of d/γ is greater than about 20, then the mechanism of transport in the support layer follows the molecular diffusion mechanism; as is the case in non-woven fabric layer.

Using Fick's first law, the vapor flux through the support layer can be written as (8):

$$J_i = \frac{D_{i,S}P_{sat,i}}{\delta_S RT}(a_{i,SM} - a_{i,P}) \tag{14}$$

Where $D_{i,S}$ is estimated by molecular diffusivity. Thus, the resistance of the support layer (non-woven fabric layer) can be written as:

$$R_{i,S} = \frac{\delta_S RT}{D_{i,S} P_{sat,i}} \tag{15}$$

If the average free path of vapor molecules is in the order of a micro meter, i.e. d/γ is smaller than about 0.2, then the Knudsen flow mechanism governs. In this case, the following equation can be written:

$$J_i = \frac{d\bar{u}_i}{3RT\delta_S}(P_{i,SM} - P_{i,P}) \tag{16}$$

Where, $\bar{u}_i$ is determined by gas kinetic theory as follows:

$$\bar{u}_i = \left(\frac{8g_c RT}{\pi M_i}\right)^{1/2} \tag{17}$$

Then, the following equations can be written:

$$J_i = \left(\frac{8g_c RT}{\pi M_i}\right)^{1/2} \frac{d}{3RT\delta_S}(P_{i,SM} - P_{i,P}) \tag{18}$$

$$P_i = P_{sat,i} a_i$$

Thus, the resistance of the support layer (PAN layer) can be written as:

$$R_{i,S} = \frac{3RT\delta_S}{d \times P_{sat,i}} \left(\frac{\pi M_i}{8RTg_c}\right)^{1/2} \tag{19}$$

Total Mass Transfer Resistance

Using Eqs. (6), (13), and (15) or (19), the total resistance can be rewritten as follows:

$$R_{i,T} = \frac{a_{i,L} - a_{i,P}}{J_i} = R_{i,L} + R_{i,M} + R_{i,S} \tag{20}$$

Estimation of Permeation Flux Passing Through the Membrane and Separation Factor

Diffusion model is on the basis of Fick's law. Generally, the mass transfer rate, in every phase, is due to moving of bulk and component itself.

$$J_i = (J_i + J_j)\phi_i - \rho D_i \frac{d\phi_i}{dz} \tag{21}$$

Assuming that $h = \frac{J_i}{J_j}$, after integration the following equation can be written:

$$J_i = \frac{\rho_i}{l} \int_0^{\phi_{i,f}} \frac{D_i}{1 - \phi_i(1 + \frac{1}{h})} d\phi_i \tag{22}$$

Note that here volume fraction is used instead of mass fraction and also when the permeate side pressure is sufficiently low, $\phi_{i,p}$ becomes zero.

The separation factor (α) can be calculated by (12):

$$\alpha = \frac{y(1-x)}{x(1-y)} \tag{23}$$

Where y and x represent the ortho_xylene concentration in permeate and feed, respectively. It must be noted that in the experiments in presence of CBr_4, y and x are the ortho_xylene concentration in the permeate and in the feed (CBr_4 free).

Determination of Volume Fraction of Component at the Feed Side Membrane Interface

Based on the solution-diffusion model, it is assumed that swelling equilibrium is reached at the interface between the feed mixture and the polymeric membrane:

$$a_i^l = a_i^m \tag{24}$$

Calculation of Activity in the Liquid Phase. Here for the liquid phase, UNIFAC model can not be used to estimate activity, because this model does not distinguish between isomeric groups. One may apply the simplest form of Gibbs excess energy, two suffixes Margules equation, for simple liquid mixtures (mixture of molecules that have the same shape,

size and chemical structure) to determine activity at the feed side membrane interface:

$$\begin{cases} x_1\gamma_1^l = a_1^l = x_1 \cdot \exp\left(\frac{A'}{RT}x_2^2\right) & (25) \\ x_2\gamma_2^l = a_2^l = x_2 \cdot \exp\left(\frac{A'}{RT}x_1^2\right) & (26) \end{cases}$$

In these equations, the only variable is the coefficient 'A'' which can be estimated by the following equation: (least – square method):

$$P_t = x_1\gamma_1^L P_1^{sat} + x_2\gamma_2^L P_2^{sat} = x_1 P_1^{sat} \cdot \exp\left(\frac{A'}{RT}x_2^2\right) + x_2 P_2^{sat} \cdot \exp\left(\frac{A'}{RT}x_1^2\right) \quad (27)$$

Calculation of Activity in the Membrane Phase. Activity of components in the membrane phase can be affected by three contributions: combinatorial part, free volume part, and residual part.

$$\ln a_i = \ln a_i^C + \ln a_i^{FV} + \ln a_i^R \quad (28)$$

For estimation of the combinatorial part, Flory-Huggins relation can be used:

$$\frac{\Delta G_M^C}{RT} = n_1 \ln \varphi_1 + n_2 \ln \varphi_2 + n_p \ln \varphi_p \quad (29)$$

The above equation can be differentiated with regard to n_1 and n_2 to obtain $\Delta\mu_i^p/RT$:

$$\frac{\Delta\mu_i^p}{RT} = \ln a_1^C = \ln \varphi_1 + \varphi_2 + \varphi_p - \varphi_2\frac{\upsilon_1}{\upsilon_2} - \varphi_p\frac{\upsilon_1}{\upsilon_p} \quad (30)$$

For estimation of the free volume part, the following relation can be used (13):

$$\ln a_i^{FV} = \ln \varphi_i^{FV} + 1 - \frac{\varphi_i^{FV}}{\omega_i} \quad (31)$$

Zhong method can be used to determine φ_i^{FV} (14):

$$\varphi_i^{FV} = \frac{\omega_i r_i}{\omega_1 r_1 + \omega_2 r_2 + \omega_p\left[0.6583 n r_p\right]} \quad (32)$$

For estimation of the residual part, a solubility parameter method which is on the basis of the Lattice theory can be applied (13):

$$\ln a_1 = \upsilon_1 \varphi_2^2 \frac{\left[(\delta_1 - \delta_2)^2\right]}{RT} \tag{33}$$

Thus, for a mixture containing three components (ortho_xylene, para_xylene, and polymer (PVA)), the following equation can be written:

$$\ln a_1^R = \frac{\upsilon_1 \varphi_p^2}{RT}\left[(\delta_1 - \delta_p)^2\right] + \frac{\upsilon_1 \varphi_2 \varphi_p}{RT}\left[(\delta_2 - \delta_p)^2\right] + \frac{\upsilon_1 \varphi_2^2}{RT}\left[(\delta_1 - \delta_2)^2\right] \tag{34}$$

In which, the solubility parameters of ortho_xylene and para_xylene are equal to 18 and that of polymer is equal to 25.78 (15). Thus, the last term in the right hand side of the above equation can be ignored. According to Eq. 24, concentration of the component at the feed side membrane interface according to a given feed composition and temperature can be determined using least-square minimization, which is minimization of the objective function, $\sum (a_i^l - a_i^m)^2$.

Determination of Mutual Diffusion Coefficient in the Membrane Phase

According to the work of Vrentas-Duda (16), mutual diffusion coefficient (D) can be related to self diffusion coefficient (D_T) using the following relationship:

$$D_i = (D_T)_i (1 - \varphi_i)\varphi_i \frac{\partial \ln a_i}{\partial \varphi_i} \tag{35}$$

Free volume theory can be used to predict the self-diffusion coefficient of small molecules through polymers (11):

$$D_T = RT\widetilde{A} \exp\left(\frac{\widetilde{B}}{f}\right) \tag{36}$$

Where, $\tilde{A}$ and $\tilde{B}$ are the parameters related the to shape and the size of the diffusing molecules. Fractional free volume, f, is a function of the volume fraction of the component i (ϕ_i) and temperature (T).

$$f(\varphi_i, T) = f(0, T) + \beta_i(T)\varphi_i \tag{37}$$

$$f(0, T) = a(T - T_g) + 0.025 \tag{38}$$

Parameter a can be set to $4.8 \times 10^{-5}\ K^{-1}$ when $T < T_g$, and $4.8 \times 10^{-4}\ K^{-1}$ when $T > T_g$. β (T) is a proportional constant which can be determined using the fractional free volume of pure liquid.

To determine the free volume parameters, $\tilde{A}$ and $\tilde{B}$, the diffusion coefficient relation in infinite dilution can be employed. If $\varphi_i = 0$, then Eq. (36) can be rewritten in the form below in which, D_i^0 is the diffusion coefficient of the infinite dilution component i in j:

$$D_i^0 = RT\widetilde{A} \exp\left(\frac{\widetilde{B}}{f(0,T)}\right) \tag{39}$$

The above equation can be equalized to Wilk-Chang equation (17), i.e.:

$$D_i^0 = \frac{7.4 \times 10^{-8}(\phi_j M_j)^{1/2} T}{\mu_j v_i^{0.6}} \tag{40}$$

With solving the resulted equation at two different temperatures, $\tilde{A}$ and $\tilde{B}$ can be calculated.

The term $\left(\frac{\partial \ln a_i}{\partial \varphi_i}\right)_{T,P}$ can be calculated by means of the activity relations achieved previously in the membrane phase.

EXPERIMENTAL AND PHYSICAL DATA

PV Experiments

PV experiments were carried out using an apparatus as shown in Fig. 2. PVA membrane purchased from Sulzer Company consisted of three layers (PVA as the dense top membrane layer with thickness of 2 μm and PAN and non-woven fabric layers as the support with thicknesses of 70 μm and 100 μm, respectively). The membrane was housed in a PV cell that consisted of two detachable stainless steel parts. The membrane had an effective area of approximately $0.0024\ m^2$. Rubber O-rings were used to provide a pressure tight seal between the membrane and the cell. A pump was employed to recirculate the feed solution in a continuous mode. Volume of feed tank was 5 L, which was very big compared with permeation volume; therefore, variation of the feed concentration during an experimental period was negligible. In all experiments, the permeate pressure was maintained at a low level (about 20 mbar) by employing a vacuum pump. Permeate samples were condensed and collected in a Pyrex glass condenser kept inside a cryogenic trap at −35°C. The permeate collected in the cold trap was weighted by a digital balance

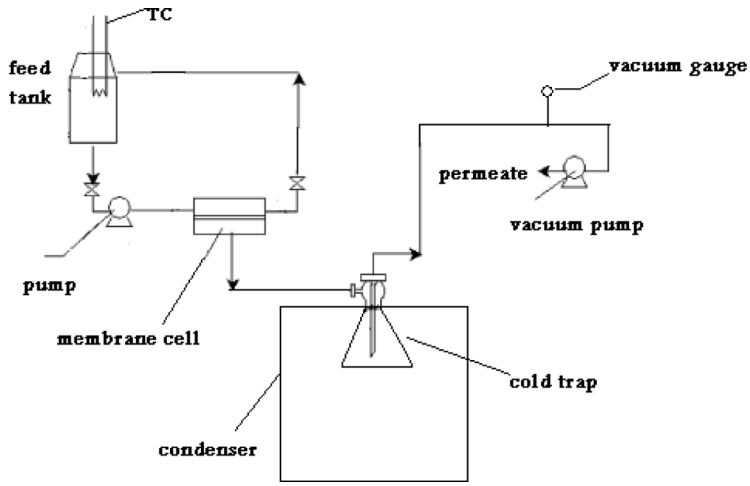

Figure 2. Schematic diagram of the experimental set-up.

within accuracy of .001 gr. The samples were then analyzed using a gas chromatography (GC model: 2010 SHIMADZU, Column Name: BP-5 (PEG), Column length: 28.5 m, Carrier Gas: He, Temperature: 300°C, Pressure: 131.3 kPa). The experiments were performed at a constant temperature of 40°C and at a feed rate of 1.755 lit/min with different para-_xylene concentrations (10–40%) and permeate pressures (20–50 mbar). Also, the experiments in the presence of CBr_4 (constant amount of 10% w/w) were carried out at different feed compositions and constant temperature and permeate pressure as the previous ones without CBr_4.

Degree of Swelling at Equilibrium

The PVA membrane after completely drying at room temperature and weighting was immersed into solutions of 10–40 wt.% para_xylene in a sealed vessel at 40°C. At equilibrium after 96 h, the membrane was rapidly taken out of the vessel, wiped quickly with filter paper to remove the solvent residue, and then reweighed. Degree of swelling, DOS, can be calculated as:

$$\mathrm{DOS} = \frac{W_s - W_d}{W_d} \times 100 \tag{41}$$

Where, W_s denotes weight of the swollen membrane and W_d denotes weight of the membrane before immersion (dry membrane).

The sorption selectivity based on the degree of swelling of pure xylenes (o_/p_xylene) is around 1.87, which is comparable with the result of literature (18). Lue et al. mentioned that the sorption selectivity is constant around 1.4.

Physical Properties Data

The physical properties required for the calculations were obtained as the following:

Viscosities of the xylene mixtures were estimated using the following equation (19):

$$\ln \eta_{\text{mix}} = \sum x_i \ln \eta_i \tag{42}$$

Densities of the xylene mixtures were also calculated using the equation similar to Eq. (42).

Saturated vapor pressures of the xylenes were calculated using the Antoine equation (19).

$$\log P = B - \frac{A}{(T + C)} \tag{43}$$

In which, A and B are experimental constants.

Mean free paths of the xylenes in the porous support were calculated using the literature (20).

$$\lambda = (n\sigma)^{-1} \tag{44}$$

In which, n is the number of target particles per unit volume, and σ is the effective cross sectional area for collision.

Diffusion coefficients of the xylene vapors in the porous support were calculated using the literature (8).

$$D_{AB} = \frac{3}{16} \frac{(4\pi kT/M_{AB})^{1/2}}{n\pi\sigma_{AB}^2 \Omega_D} f_D \tag{45}$$

In which n = number density of molecules in the mixture,
k = Boltzmann's constant
Ω_D = diffusion collision integral, dimensionless
σ_{AB} = characteristic length, A°

Diffusion coefficients of the xylenes were calculated using the Vignes equation (20).

$$D_{AB}\eta = \left[\left(D_{AB}^0 \eta_B \right)^{x_B} \left(D_{BA}^0 \eta_A \right)^{x_A} \right] \alpha \tag{46}$$

In which $\alpha = \left[\frac{(\partial \ln a_A)}{(\partial \ln x_A)}\right]_{T,P}$

Viscosities of the xylene vapors were estimated using the following equations (19)

$$\mu_{\text{mix}} = \sum_{i=1}^{k} \frac{x_i \mu_i}{\sum_{j=1}^{k} x_j \Phi_{ij}} \tag{47}$$

$$\Phi_{ij} = \left(\frac{1}{8^{1/2}}\right)\left(1 + \frac{M_i}{M_j}\right)^{-1/2}\left[1 + \left(\frac{\mu_i}{\mu_j}\right)^{1/2}\left(\frac{M_i}{M_j}\right)^{1/4}\right]^2 \tag{48}$$

The volume parameters for the solution and monomer of polymer (r_1, r_2, r_p) were calculated using the literature (19).

Solubility parameters (δ_i) were calculated using the literature (15).

RESULTS AND DISCUSSION

Swelling of PVA Membrane in Para_xylene/Ortho_xylene Mixtures

Results of the swelling measurements in para_xylene/ortho_xylene binary mixtures are shown in Table 1. Degree of swelling of the PVA membrane was measured as a function of para_xylene concentration. Results show that the amount of absorption decreases with increasing para_xylene concentration. This means that ortho_xylene more swells the PVA membrane than para_xylene, because para_xylene is slightly less polar than ortho_xylene and also the PVA membrane has a hydrophilic characteristic (Log $K_{ow} = 3.01$ for ortho_xylene and 3.15 for para_xylene).

PV Results

Effect of Feed Concentration

Table 2 represents that the total permeation flux decreases with increasing para_xylene concentration in the feed (without CBr_4) for all mixtures studied. The results are comparable with the results of the work of Chen et al. (22). It is due to the fact that with decreasing ortho_xylene

Table 1. Degree of swelling of PVA membrane

Para_xylene concentration in feed (wt %)	0	10	20	30	40	100
Degree of swelling (DOS)	0	0.71	0.66	0.5	0.47	0.38

Table 2. Effect of concentration on experimental and calculated total flux and para_xylene and ortho_xylene fluxes ($P_2 = 20$ mbar)

Para_xylene concentration in feed (wt %)	10	20	40
Total flux (g/m2.h) (experimental)	803.21	665.2	382.5
Total flux (g/m2.h) (calculated)	836.5	7566	669
P_xylene flux (g/m^2.h) (experimental)	73.9	115.21	116.66
O_xylene flux (g/m^2.h) (experimental)	729.31	550	265.83

concentration in the feed, the amount of its sorption into the membrane decreases, and as a result, the membrane becomes less swollen. As seen in Table 2, total permeation flux predicted by the proposed model (Eq. (22)) is in good agreement with the experimental data at lower para_xylene concentrations. The main parameters associated with the modeling equation are diffusion coefficient, density and volume fraction of the components at the feed side membrane interface. The errors may come from the supposed swelling equilibrium (Eq. (24)), which may not to be attained in the experiments. In fact, at higher concentrations (40 wt% para_xylene), the degree of non-equilibrium (i.e. non equality of activities in interface between the feed mixture and the polymeric membrane) is more significant (11). Ortho_xylene and para_xylene permeation fluxes (experimental) are also presented in Table 2. As seen, the para_xylene flux increases and the ortho_xylene flux decreases with increasing

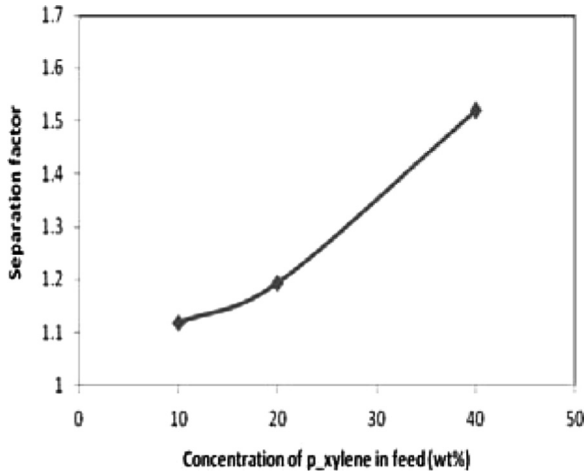

Figure 3. Effect of concentration on ortho_xylene separation factor (experimental) ($P_2 = 20$ mbar).

para_xylene concentration in the feed. In Fig. 3, ortho_xylene separation factor as a function of para_xylene concentration in the feed can be observed. This figure shows that the separation factor increases with increasing para_xylene concentration in the feed. With increasing para_xylene concentration in the feed, its permeation through the membrane decreases, and thus, the separation factor (ortho_xylene versus para_xylene) increases. This phenomenon can be related to interaction forces of the xylene molecules in transfer process inside the polymer, which results in rapid transfer of ortho_xylene molecules compared with para_xylene molecules through the membrane phase. The absolute amounts of separation factors achieved in this work are in the range of 1.1 to 1.8, which are comparable with the results attained by Chen et al. (22) that are in the range of 1.2 to 1.75. The transport mechanism of xylene isomers through the PVA membrane is governed by the solution-diffusion model. The permeation rate is related to the combined effects of solubility and diffusivity. As mentioned in section 3.2, the sorption selectivity (o_/p_xylene) is about 1.87. Also, the order of magnitude of diffusion coefficients is 10^{-6}. Thus; the diffusion selectivity (o_/p_xylene) lene) can be around 0.82. This implies that the effect of solubility is greater than that of diffusivity in this case of permeation selectivity.

Effect of Permeate Pressure

Table 3 shows that reduction of permeate pressure in the studied range does not have any considerable effect on total permeation flux. Effect of permeate pressure on para_xylene and ortho_xylene permeation fluxes are also presented in Table 3. Also, Fig. 4 presents the effect of permeate pressure on the ortho_xylene separation factor. As seen, ortho_xylene permeation flux increases and para_xylene permeation flux almost remains constant with reduction of the permeate pressure. Usually, decreasing permeate pressure results in higher pressure difference, and as a result,

Table 3. Effect of permeate pressure on total flux and para_xylene and ortho_xylene fluxes (experimental) (para_xylene concentration in the feed = 20 wt %)

Permeate pressure (mbar)	20	35	48
Total flux ($g/m^2.h$) (experimental)	665.2	651.04	648.3
Total flux ($g/m^2.h$) (Calculated)	756	736	698
P_xylene flux ($g/m^2.h$) (experimental)	114	117	122
O_xylene flux ($g/m^2.h$) (experimental)	548	532	523

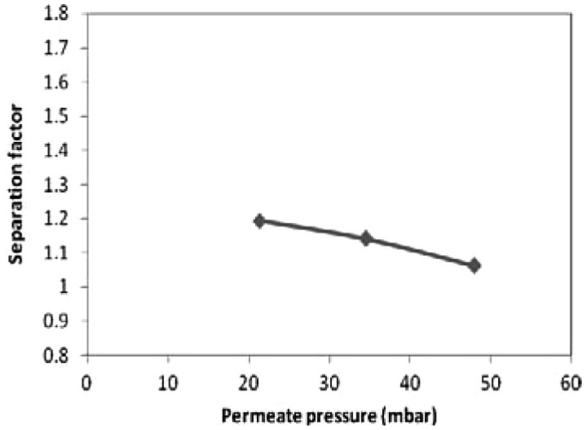

Figure 4. Effect of permeate pressure on ortho_xylene separation factor (experimental) (para_xylene concentration in feed = 20 wt %).

higher driving force. However, the flux enhancement depends on the thermodynamic properties of organic constituents like saturated vapor pressure and activity coefficient. Due to this fact and regarding Eq. (49), it can be said that when saturated vapor pressure and the activity coefficient are sufficiently large, small variations of permeate pressure in limited ranges may have an insignificant influence on total driving force and permeation flux (21).

$$J_i = \frac{D_i P_i^{sat}}{l}\left(\gamma_i x_i - \frac{P_i}{P_i^{sat}}\right) \tag{49}$$

Mass Transport Resistances

All the resistances calculated were positive except for the liquid boundary layer resistance for para_xylene. This shows that the transport of para_xylene is in the opposite direction compared with that of ortho_xylene in the boundary layer zone. Variations of all resistances as functions of feed concentration and permeate pressure are shown in Figs. 5 and 6, respectively. As seen, the liquid boundary layer resistance to transport of para_xylene ($R_{p,L}$) is higher than that of ortho_xylene ($R_{o,L}$). This demonstrates the higher permeation rate of ortho_xylene through the membrane. $R_{o,L}$ remains relatively constant with increasing para_xylene concentration in the feed. Also, the membrane top layer resistance to transport of para_xylene ($R_{p,M}$) is greater than that of ortho_xylene

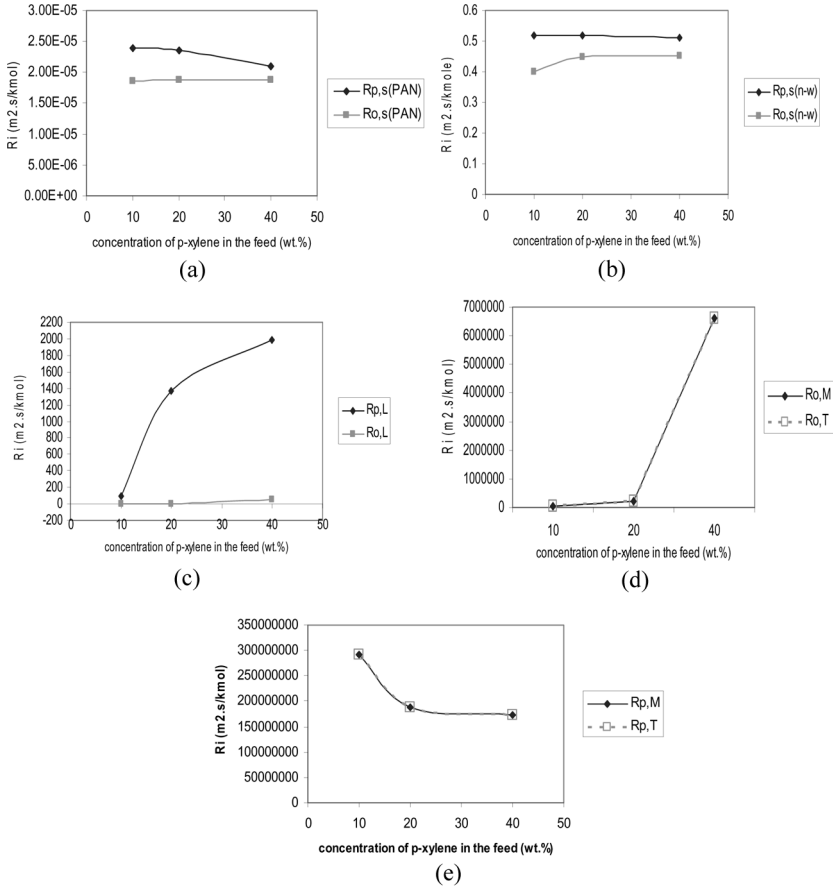

Figure 5. Effect of para_xylene concentration on (a) PAN support layer resistance; (b) non-woven fabric support layer resistance; (c) liquid boundary layer resistance; (d) membrane top layer resistance and total resistance for ortho_xylene; (e) membrane top layer resistance and total resistance for para_xylene.

($R_{o,M}$). Finally, the membrane porous support layer resistance to transport of para_xylene ($R_{p,S}$) is greater than that of ortho_xylene ($R_{o,S}$).

By comparison of the three resistances in the liquid boundary layer, the membrane top layer and the membrane support layer, one can observe that the membrane top layer resistance is the highest. As a result, it can be confirmed that the membrane top layer resistance ($R_{o,i}$) controls transport in this case of study. Accordingly, it can be said that the membrane porous support layer resistance (PAN layer) is negligible.

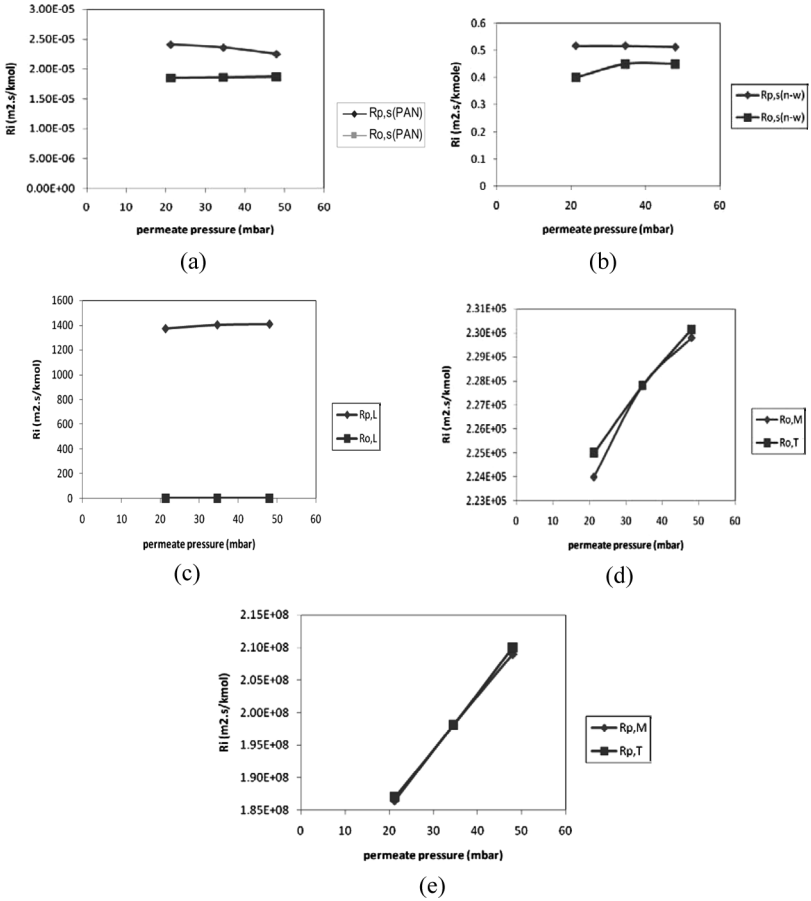

Figure 6. Effect of permeate pressure on (a) PAN support layer; (b) non-woven fabric support layer; (c) liquid boundary layer; (d) membrane top layer and total for ortho_xylene; (e) membrane top layer and total for para_xylene resistances.

PV in the Presence of CBr_4

In the presence of CBr_4, the overall separation process tends to be more selective for ortho_xylene. Experiments were carried out using feed mixtures containing 20%, 50%, and 80% para_xylene in ortho_xylene in which 10 wt.% CBr_4 (based on the total volume), was solubilized. The results of these experiments are presented in Fig. 7. Comparing with Table 2 and Fig. 3, one can see the reduction of the total flux in the presence of CBr_4 in the feed. However, increasing para_xylene concentration

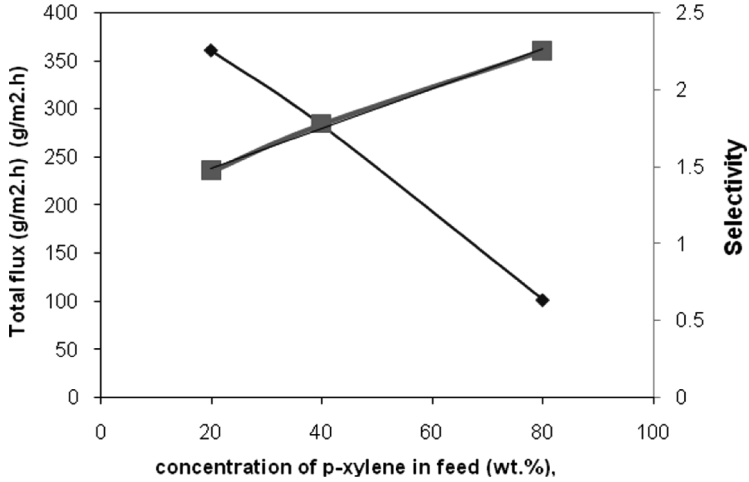

Figure 7. Effect of CBr_4 on PV of isomeric xylenes.

in the feed (in the presence of CBr_4) increases the ortho_xylene separation factor. This is because of the fact that CBr_4 combines with para_xylene and the resulting compound is less permeable through the membrane, and thus, more ortho_xylene passes through the membrane (10). It has to be noted that, on the basis of permeate analysis, there was only a trace amount of CBr_4 in the permeate.

CONCLUSIONS

The resistances-in-series model with a modified solution-diffusion model was used to calculate the main three resistances of isomeric xylene molecules as well as the permeation flux through the membrane. For PV of ortho_xylene and para_xylene mixtures using a composite PVA membrane, mass transport of the system was found to be governed by the transport resistance of constituents in the membrane top layer ($R_{p,M}$, $R_{o,M}$). On the other hand, transport resistances in the membrane porous support layer were found to be negligible. All transport resistances for ortho_xylene were found to be lower than those for para_xylene. Analyses of the permeation flux showed that the total flux calculated by the proposed model is in good agreement with the experimental data at lower feed concentrations. PV under conditions where there is a selective compound formation with CBr_4 results in a process that is relatively more selective for ortho_xylene. In other words, the para-xylene complex is retained on the feed side of the membrane via the selective compound

formation. It has to be finally concluded that the separation of ortho_xylene and para_xylene mixtures can be effectively performed using pervaporation.

SYMBOLS

a_i	activity of component i
$a_{i,X}$	activity of component i in X bulk
$a_{i,XY}$	activity of component i in X at X/Y interface
a_i^C	activity of component i from combinatorial contribution
a_i^{FV}	activity of component i from free volume contribution
a_i^R	activity of component i from residual contribution
a_i^l	activity of component i in the feed
a_i^m	activity of component i in the feed side surf ace of the membrane
$c_{i,X}$	molar concentration of component i in X (kmol/m^3)
d	pore diameter (m)
D_i	mutual diffusion coefficient in the membrane (m^2/s)
$D_{i,X}$	diffusion coefficient of component i in X (m^2/s)
$Di_{i,M}{}^0$	diffusion coefficient of component i in the membrane at infinite dilution (m^2/s)
g_c	gravitational constant (m/s^2)
ΔG_M^C	Gibbs free energy of ternary mixture (binary liquid and polymer in polymer phase)
J_i	molar flux of component i (mol/m^2.h)
k	number of species in the mixture
k_{bl}	mass transfer coefficient in liquid boundary layer (m/s)
k_{ii}	plasticizing coefficient of component i for two-component permeation (m^3/kmol)
k_{ij}	coupling coefficient of component i with j (m^3/kmol)
K_{si}	sorption coefficient of component i (kmol/m^3)
l	the composite membrane thickness (m)
M_i	molecular weight of component i (kg/kmol)
n	monomer number in a chain molecule
n_i	mole numbers of component i
$p_{sat,i}$	saturated vapor pressure of component i (kg/m.s^2)
P_t	total pressure (kg/m·s^2)
Pi	partial vapor pressure of component i (kg/m.s^2)
$P_{i,X}$	partial vapor pressure of component i in X (kg/m.s^2)
$P_{i,XY}$	partial vapor pressure of component i in X at X/Y interface (kg/m.s^2)
r_i	relative volume parameter of component i

r_p	volume parameter for the membrane (monomer)
R	ideal gas constant
Ri, L	liquid boundary layer resistance of component i (m^2.s/kmol)
Ri, M	membrane top layer resistance of component i (m^2.s/kmol)
Ri, S (PAN)	support layer (PAN) resistance of component i (m^2.s/kmol)
Ri, S (n-w)	support layer (non woven fabric) resistance of component i (m^2.s/kmol)
Ri, T	total resistance of component i (m^2.s/kmol)
T	temperature (K)
Tg	glass transition temperature (K)
$\bar{u_i}$	mean molecular velocity of i (m/s)
V_p	velocity in boundary layer perpendicular to membrane surface (m/s)
xi	mole fraction of component i
$x_{i,X}$	mole fraction of component i in X
Z	coordinate perpendicular to membrane surface (m)
ϕ_i	volume fraction term of component i
ρL	molar density of liquid feed (kmol/m^3)
η_i	viscosity of pure i (aqueous) (pa.s)
η_{mix}	viscosity of the mixture (aqueous) (pa.s)
μ_i	viscosity of pure molecules at the T and P of the mixture (vapor) (pa.s)
μ_{mix}	viscosity of the mixture (vapor) (pa.s)
δ	solubility parameter of component i
δ_M	membrane thickness (m)
δ_S	porous support thickness (m)
γ_i	activity coefficient
υ_i	molar volume of component i (m^3/kmol)
$\Delta\mu_i^p$	chemical potential of component i in polymer phase
ω_i	mass fraction of component i
λ	mean free path of xylene molecules
Subscripts	
L	liquid
M	membrane
P	permeate
S	support
X	liquid (L), membrane (M), permeate (P), or support (S)
Y	liquid (L), membrane (M), permeate (P), or support (S)
p	polymer

REFERENCES

1. Kusumocahyo, S.P.; Kanamori, T.; Sumaru, K.; Iwatsubo, T.; Shinbo, T. (2004) Pervaporation of xylene isomer mixture through cyclodextrins containing polyacrylic acid membranes. *J. Membr. Sci.*, *231*: 127–132.
2. Smitha, B.; Suhanya, D.; Sridhara, S.; Ramakrishna, M. (2004) Separation of organic–organic mixtures by pervaporation—a review. *J. Membr. Sci.*, *241*: 1–21.
3. Sikonia, J.G.; McCandless, F.P. (1978) Separation of isomeric xylenes by permeation through modified plastic films. *J. Membr. Sci.*, *4*: 229–241.
4. Wegner, K.; Dong, J.; Lin, Y.S. (1999) Polycrystalline MFI zeolite membranes: Xylene pervaporation and its implication on membrane microstructure. *J. Membr. Sci.*, *158*: 17–27.
5. Takaba, H.; Douglas Way, J. (2003) Separation of isomeric xylenes using cyclodextrin-modified ceramic membranes. *Ind. Eng. Chem. Res.*, *42*: 1243–1252.
6. Chen, H.L.; Wu, L.G.; Tan, J.; Zhu, C.L. (2000) PVA membrane filled β-cyclodextrin for separation of isomeric xylenes by pervaporation. *Chem. Eng. J.*, *78*: 159–164.
7. Jiraratananon, R.; Chanachai, A.; Huang, R.Y.M. (2002) Pervaporation dehydration of ethanol-water mixtures with chitosan/hydroxyethy cellulose (CS/HEC) composite membranes: Analysis of mass transport. *J. Membr. Sci.*, *199*: 211–222.
8. Liu, M.G.; Dickson, J.M.; Cote, P. (1996) Separation of a pervaporation system on the industrial scale for water treatment part 1: Extended resistance-in-series model. *J. Membr. Sci.*, *111*: 227–241.
9. Peng, F.; Pan, F.; Li, D.; Jiang, Zh. (2005) Pervaporation properties of PDMS membranes for removal of benzene from aqueous solution: Experimental and modeling. *Chem. Eng. J.*, *114*: 123–129.
10. Wytcherley, R.W.; McCandless, F.P. (1992) The separation of meta- and para-xylene by pervaporation in the presence of CBr_4, a selective feed complexing agent. *J. Membr. Sci.*, *67*: 67–74.
11. Burn, J.P.; Larchet, C.; Melet, R.; Bulvestre, G. (1985) Modelling of the pervaporation of binary mixtures through moderately swelling, non-reacting membranes. *J. Membr. Sci.*, *23*: 257–283.
12. Bakhshi, A.; Mohammadi, T.; Ghaffari Nik, O.; Aroujalian, A. (2006) Effect of operating conditions on pervaporation of methanol-water mixtures: Part 2. *membrane technology*, December: 7–11.
13. Prauznitz, J.M.; Lichtenthaler, R.N.; de Azevedo, E.G. (1999) *Molecular Thermodynamics of Fluid-Phase Equilibria*, 3rd Ed., Prentice Hall PTR.
14. Zhong, C.; Sato, Y. (1980) Improvement of predictive accuracy of the UNIFAC model for vapor-liquid mixtures. *J. Chem. Eng.*, *58*: 253–258.
15. Brandrup, J.; Immergut, E.H. (1989) *Polymer Handbook*, 3rd Ed. Wiley: New York, 102. Greenley, ZR.
16. Kim, J.S.; Lee, K.R. (2000) Prediction of mutual diffusion coefficient in polymer solution. *Polymer*, *41*: 8441–8448.

17. Perry, R.H.; Green, D. (1977) *Perry's Chemical Engineers' Handbook*; 6th Ed. McGraw-Hill: New York.
18. Lue, Sh. J.; Liaw, T. (2006) Separation of xylene mixtures using polyurethane- zeolite composite membranes. *Desalination*, *193*: 137–143.
19. Reid, R.C.; Prausnitz, J.M.; Sherwood, T.K. (1977) *The Properties of Gases and Liquids*, 3rd Ed., McGraw-Hill: New York.
20. Treybal, R.E.. (1990) *Mass Transfer Operations*; 3rd Ed., McGraw-Hill: Tokyo.
21. Madandar, A.; Mohammadi, T. (2006) Effect of permeate pressure on pervaporation of methyl tert-butyl ether/methanol mixtures. *Desalination*, *200*: 390–392.
22. Chen, H.L.; Wu, L.G.; Tan, J.; Zhu, C.L. (2000) PVA membrane filled β-cyclodextrin for separation of isomeric xylenes by pervaporation. *Chem. Eng. J.*, *78*: 159–164.